

# Noise characteristics and detectivity of $\text{YBa}_2\text{Cu}_3\text{O}_{7-x}$ superconducting bolometers: Bias current, frequency, and temperature dependence

M. Fardmanesh, A. Rothwarf, and K. J. Scoles

*Drexel University, Electrical and Computer Engineering Department,  
and Ben Franklin Superconductivity Center, Philadelphia, Pennsylvania 19104*

(Received 2 June 1995; accepted for publication 9 November 1995)

Meander line patterned infrared detectors, with values of resistance  $R_{\text{onset}}$  at the onset temperature  $T_{c \text{ onset}}$  of 3–5 k $\Omega$ , were fabricated from  $\text{YBa}_2\text{Cu}_3\text{O}_{7-x}$  superconducting material on MgO and  $\text{SrTiO}_3$  crystalline substrates. Noise voltages from the samples were measured versus bias current, radiation modulation frequency, and temperature, in both the normal and superconducting states. Four major types of voltage noise were identified according to where they occurred in temperature relative to  $T_{c \text{ onset}}$  and the zero resistance temperature  $T_{c \text{ zero}}$ , and their dependence on frequency and bias current. They were also associated with the granularity of the superconducting film, which is related to the substrate material used. From these observations a specific cause for each type of noise is suggested. The results are as follows. (i) In the normal state with temperature  $T > T_{c \text{ onset}}$ , noise with a magnitude that is consistent with thermal (Johnson) noise is seen, but it depends linearly on bias current above a threshold value, at low frequencies. The suggested noise source is conductivity fluctuations due to Cooper pairs. (ii) Noise was found to occur below  $T_{c \text{ zero}}$  in granular films. With increasing bias current its magnitude increases, and it shifts to a lower temperature range; however, the noise magnitude becomes constant as the current goes to zero. It is weakly dependent on frequency above 400 Hz. Suggested cause is voltage fluctuations in superconductor–normal–superconductor junctions at grain boundaries. (iii) This noise also occurs below  $T_{c \text{ zero}}$  with peaks at various temperatures. With increasing bias current the peaked noise spreads to lower temperatures, but the noise goes to zero as the bias current goes to zero. Its suggested cause is magnetic flux tube motion. (iv) This noise occurs between  $T_{c \text{ onset}}$  and  $T_{c \text{ zero}}$  and is present in all samples, but lowest on samples prepared on  $\text{SrTiO}_3$  substrates. Its suggested cause is fluctuations in the volume fraction of the superconducting phase along the current path. While the measured detectivity  $D^*$  of our samples at a wavelength of 20  $\mu\text{m}$  was only  $10^6 \text{ cm Hz}^{1/2}/\text{W}$ , engineering changes can be expected to raise the value to above  $10^{10} \text{ cm Hz}^{1/2}/\text{W}$ . © 1996 American Institute of Physics. [S0021-8979(96)03904-8]

## I. INTRODUCTION

### A. Infrared radiation detector characteristics

Noise characteristics, which depend on the operating temperatures, bias current, and modulation frequency, determine the ultimate sensitivity of a superconducting bolometer.<sup>1</sup> The responsivity, defined as the output signal per watt of input signal, is important in that one wishes to detect the smallest possible signals, limited by noise from the detector. The noise equivalent power (NEP), defined as the input signal power that would give the noise observed in the output, together with the responsivity determine the detectivity  $D^*$  as given in Eq. (1). Ultimate performance in a detection system is achieved when the noise generated by the background photon flux incident on the detector is larger than any thermally generated noise within the detector.<sup>2</sup>

The detectivity versus temperature can be written as a function of the responsivity and the noise, as

$$D^* = \frac{\sqrt{A(\Delta f)r_v}}{V_n}, \quad (1)$$

where  $A$  is the radiation absorbing area of the detector,  $r_v$  is the responsivity,  $V_n$  is the voltage noise, and  $\Delta f$  is the frequency range used to obtain the noise measurement. The detectivity of superconducting transition bolometers is a

function of the bias temperature through the slope of the resistance versus temperature curve  $dR/dT$  and the bias current, since  $r_v$  is proportional to these.<sup>1</sup> It also depends on the modulation frequency since  $r_v$  depends on frequency.<sup>1</sup> To determine the best operating point for a detector one<sup>3</sup> needs to determine the dependence of  $V_n$  on temperature, bias current, and frequency.

### B. Noise in high- $T_c$ superconducting materials

There has been considerable work on the noise characteristics of superconducting materials, most of which has been focused on the low-frequency,  $1/f$  flicker noise. The study of noise in the high- $T_c$  materials may give important information about the physics of the transition.<sup>3,4</sup> This includes the onset of the several stages of the transition, the intergrain critical currents, the effect of magnetic fields, the role of inhomogeneities and other kinds of disorder, and the dynamics of the vortex motion in the material.<sup>5</sup> Noise associated with conductivity fluctuations (or resistance fluctuations)<sup>6,7</sup> has the following characteristic:

- No noise is found in the superconducting state well below  $T_c$ ;
- in the normal state near  $T_c$ , the noise is large compared to metal–insulator composites; and

TABLE I. The measured dimensions of the YBCO film patterns, superconducting characteristics, and the substrate thicknesses. The dimension of the substrates is about  $0.5 \times 1 \text{ cm}^2$  for all the samples.  $d_f$  is the thickness of the film,  $d_s$  is the thickness of the substrate,  $A$  is the total area of the pattern, and the resistance of the sample is given at room temperature ( $T=300 \text{ K}$ ).

Sample number	Substrate material	$d_f$ (nm)	$d_s$ (cm)	$A$ ( $\text{cm}^2$ )	Active area of the pattern	$R$				$G$ (W/K)
						( $T=300 \text{ K}$ )	$R_{\text{onset}}$ (k $\Omega$ )	$T_{c \text{ zero}}$ (K)	$T_{c \text{ onset}}$ (K)	
064-01a	SrTiO <sub>3</sub>	220–230	0.05	0.0168	50 $\mu\text{m} \times 1.9 \text{ cm}$	10.0	2.6	79	82	$3 \times 10^{-3}$
064-02b	MgO	120–130	0.025	0.0168	50 $\mu\text{m} \times 1.9 \text{ cm}$	11.2	4.5	74	86	$15.5 \times 10^{-3}$
064-03b	MgO	170–180	0.05	0.0168	50 $\mu\text{m} \times 1.9 \text{ cm}$	6.5	2.7	69	83	$5.1 \times 10^{-3}$

(c) the noise was reported to increase in the transition region.<sup>5</sup>

The effect of a defect can be modeled as a two-level fluctuator (TLF) moving between two energy states separated by an energy barrier.<sup>8</sup> Transitions between the two states generate a random telegraph signal (RTS). Among the various mechanisms that can be responsible for such a signal in a current biased high- $T_c$  film are charge trapping and flux hopping mechanisms, which have different origins. The noise voltage associated with two-level fluctuators is frequently observed at temperatures right below  $T_c$ , and seems to be one of the universal features of these materials.<sup>9,10</sup>

An anomalous increase in low-frequency,  $1/f$ , noise for epitaxial, and granular high-temperature superconductors has been reported for temperatures close to the superconducting transition temperature.<sup>11–15</sup> There is general agreement on the observation of excess noise in granular and  $a$ - and  $c$ -axes mixed orientation  $\text{YBa}_2\text{Cu}_3\text{O}_7$  (YBCO) superconducting films, compared to high-quality epitaxial  $c$ -axis-oriented films.<sup>16,17,12,13</sup> Two ideas form the basis of the proposed interpretations of the above phenomenon: a percolating network made of superconductor and normal elements,<sup>18–20</sup> and the random motion of magnetic flux tubes.<sup>21–23</sup>

Above  $T_c$ , the Cooper pairs have a finite lifetime, and the conductivity is the sum of the conductivity of the normal electrons and the conductivity of Cooper pairs. Hence, the conductivity fluctuations in this region can be interpreted to be due to the fluctuations in the mobility and/or density of the carriers. In the lower part of the transition, another type of conductivity fluctuation is reported to be dominant. It is interpreted as fluctuations of the volume fraction of the superconducting phase.<sup>24</sup>

One of the major sources of noise in these materials is the motion of flux tubes or current vortices, which can be generated by an external magnetic field, by the self-field produced by current in the material, or spontaneously as pairs of oppositely oriented flux tubes. A noise study in the low-field, or isolated vortex, regime, in high- $T_c$  materials has shown the importance of vortex motion in low-frequency noise, which is proposed to be due to thermally activated two-level or diffusive vortex motions.<sup>25,26</sup>

Other mechanisms such as phase slip, a strong Lorentz force due to an applied current, and localized weak pinning centers have also been reported to be strongly related to the above noise characteristics.<sup>27,28</sup> It can be argued that the corresponding voltage noise at the transition temperature could

be generated by the rearrangement of vortices collectively pinned by the film microstructure, which has been shown to be affected, and partly controlled by the external field.<sup>29</sup>

In this work we discuss results from the measurements of several types of noise with different frequency, temperature, and bias current dependences. Noise measurements versus temperature and bias currents are presented, and possible governing mechanisms for the noise behavior of the samples are proposed and discussed. For the SrTiO<sub>3</sub> substrate sample, both the spectral response<sup>30</sup> and noise were measured, and from these the spectral detectivity of the sample was obtained. From the above results and the frequency response of the sample<sup>1,30</sup> one can project a maximum detectivity for an optimally designed bolometer. In addition, the noise seen in all the regions can serve as a sensitive characterization tool for superconducting thin films.

## II. SAMPLE PREPARATION AND EXPERIMENTAL SYSTEM

Infrared detectors were designed and fabricated from *in situ* deposited  $\text{YBa}_2\text{Cu}_3\text{O}_{7-x}$  superconducting films on 0.05- and 0.025-cm-thick MgO and SrTiO<sub>3</sub> crystalline substrates. The deposition was by dc off-axis magnetron sputtering with no buffer layers, at a rate of about 10 Å in, and with a substrate temperature of 720 °C. The target was stoichiometric  $\text{YBa}_2\text{Cu}_3\text{O}_7$ . Sputtering power was 75 W, sputtering pressure 250 mTorr (base pressure  $2 \times 10^{-6}$  Torr) with argon flow 75 sccm and oxygen flow 25 sccm. After deposition the substrates were cooled at 4.5 °C/min, with the system vented to pure oxygen when the temperature reached 640 °C, and then remained in pure oxygen at 450 °C for 30 min. The samples were patterned using standard photolithography, and etched in 0.75% dilute phosphoric acid. The thicknesses and dimensions of the films and the substrates are given in Table I, and the patterning process and other deposition parameters are in Ref. 1. Measurements of the noise voltage in the bolometers were carried out with an automated characterization system.<sup>1</sup> The measurements were done with a lock-in amplifier (PAR 5204) working with an effective bandwidth equivalent to 1 Hz. A lantern or sol-gel battery, with a low-noise metal-film resistor, was the current source for the measurements of the noise voltage, using a four-probe configuration. The resistor was chosen to be at least 20 times the normal resistance of the sample. An ultralow-noise preamplifier (model 030B, Perry Amplifier), with a noise limit of 0.4 nV/Hz<sup>1/2</sup>, amplified the voltage signals. The modulated infra-

TABLE II. Summary of noise characteristics.  $T_{c \text{ zero}}(I)$  is the temperature at which the resistance falls to zero as a function of the dc bias current  $I$ .

Noise type	Temperature range	Samples showing effect	Dependence on current $I$	Dependence on frequency $f$	Material properties related to noise	Suggested mechanism	Relevant figure numbers
(i)	$T > T_{c \text{ onset}}$	All	$V_n \sim C_1 + C_2 I$	weak	intrinsic to phase transitions	Cooper pair fluctuations	2,5
(ii)	$T < T_{c \text{ zero}}(I)$	064-02b on MgO	$V_n \sim C_1 + C_2 I$	weak for $f > 400$ Hz	granular structure	SNS junctions at grain boundaries	1,2,3,4
(iii)	$T < T_{c \text{ zero}}(I)$	064-03b on MgO and 064-010 on SrTiO <sub>3</sub>	$V_n \sim C_2 I$	$f^{-1}$ , Hz	normal state resistivity	flux tube motion	6,7
(iv)	$T_{c \text{ zero}} < T < T_{c \text{ onset}}$	All	$V_n \sim I$	$f^{-1}$ , $f < 400$ Hz	stoichiometry of sample	variation in superconducting phase	2,3,6,7

red radiation source was a light-emitting diode (LED) (HFE 4020, Honeywell) with peak intensity at a wavelength of 0.85  $\mu\text{m}$ , and was driven by an oscillator. The maximum intensity of the IR radiation at the sample was 2.5  $\text{mW}/\text{cm}^2$ .

### III. EXPERIMENTAL RESULTS AND DISCUSSION

The devices studied have been reported in Refs. 30 and 31 in regard to how the responsivity  $r_\nu$  in Eq. (1) depends on frequency, temperature, interface effects, bias current effects, and changes in conductance and specific heat with temperature and frequency. Here we select from the samples those which exhibit various types of noise. Table II lists the four types of noise that we have identified in our samples, the sample characteristics that we think are responsible for the noise, the region of temperature where the noise occurs, and the dependence of the noise on frequency, and dc bias current. The figures show the experimental results of the noise measurements for the different types of noise.

In Fig. 1 we show a comparison of the  $dR/dT$  curve and the IR response of the bolometer superimposed to show the presence of a noise signal below  $T_{c \text{ zero}}$ , which is comparable in size to the bolometric IR response, and is independent of the IR radiation.

The results from the noise measurements at different radiation modulation frequencies and temperatures are given in Fig. 2. From the noise characteristics measured versus tem-

perature as shown in the figure, the noise in this material can be identified with three temperature regions and three types of noise. One is type (ii) excess noise at and below  $T_{c \text{ zero}}$ , a second is type (iv) noise that follows the resistance versus temperature transition, and the third occurs and is type (i) noise above  $T_{c \text{ onset}}$ . As shown in Fig. 2, type (ii) excess noise is not significantly affected by the frequency for frequencies above 400 Hz. The magnitude of this noise is a few orders of magnitude higher than the calculated Johnson or thermal noise, and phonon noise.<sup>1</sup> The Johnson noise is calculated for a 1 Hz bandwidth from

$$V_{\text{John}} = \sqrt{4k_B T R}, \quad (2)$$

where  $k_B$  is Boltzmann's constant,  $T$  is the temperature, and  $R$  is the resistance of the sample at the temperature indicated. The resistances and thermal conductances of the samples are given in Table I. The phonon noise is calculated from

$$V_{\text{phonon}} = r_\nu \sqrt{4Gk_B T^2}, \quad (3)$$

where  $G$  is the thermal conductance of the sample and  $r_\nu$  its responsivity.

#### A. Type (i) noise

The effect of the bias current on the noise in the normal region above  $T_{c \text{ onset}}$  has been investigated. This noise is found to be consistent with Johnson noise at this temperature, but is found to be current dependent at low frequencies as reported by other groups.<sup>16,17,29</sup> The dependence of the

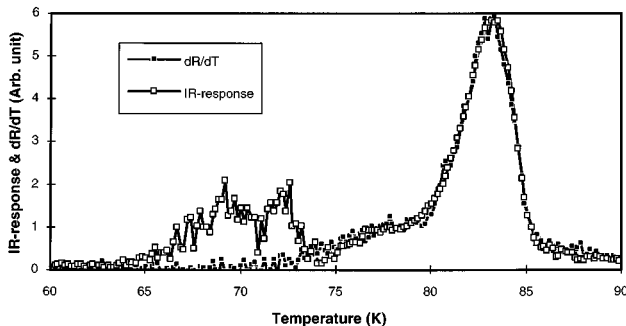


FIG. 1. IR response and resistance vs temperature of sample 064-02b, on MgO, at a bias current of 100  $\mu\text{A}$  and at a modulation frequency of the IR radiation of 10 kHz. The response below 74 K ( $T_{c \text{ zero}}$ ) is a noise signal that is independent of the IR radiation.

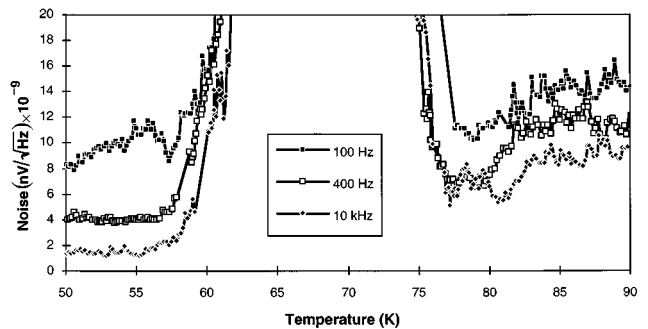


FIG. 2. Noise voltage vs temperature of sample 064-02b, on MgO, at 100  $\mu\text{A}$  bias current for 100 Hz, 400 Hz, and 10 kHz modulation frequencies.

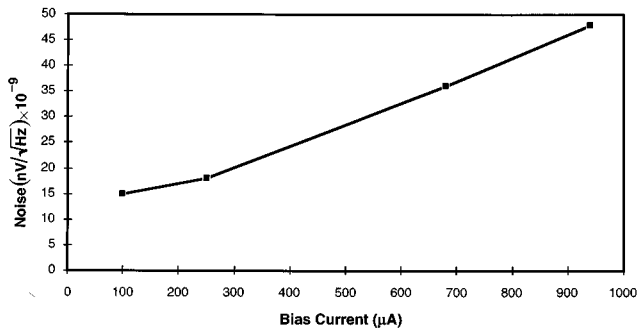


FIG. 3. Noise voltage vs bias current for sample 064-02b, on MgO, at 100 Hz at temperatures between 90 and 100 K.

noise on the bias current suggests that the noise can be due to the resistance fluctuations in the material. The noise voltage of sample no. 064-02b in the normal state close to  $T_{c \text{ onset}}$  was measured at different bias currents, and is given in Fig. 3. The noise voltage is linearly proportional to the bias current for values above about 200  $\mu\text{A}$ . This suggests that the noise in the normal state is caused by resistance or conductivity fluctuations in the film, and also suggests that the resistance (or conductivity) fluctuations are not dependent on the bias current. Above the transition temperature, the Cooper pairs have a finite lifetime, and the conductivity is the sum of the conductivity of the normal electrons and the conductivity of Cooper pairs, which can fluctuate randomly. Hence, the conductivity fluctuations in this region can be interpreted to be due to the fluctuations in the density of the different types of the carriers.<sup>32</sup>

### B. Type (ii) noise

The dependence of the noise voltage on bias current at temperatures less than  $T_{c \text{ zero}}$  was investigated and the results at 10 kHz frequency, shown in Fig. 4, indicate that the region in temperature where noise is present widens with an increase in the bias current, and goes to lower temperatures at higher currents. This is thought to be due to the presence of weak links and their associated superconductor-normal-superconductor (SNS) junctions. The broadening of the noise region in temperature with an increase in current can be interpreted as due to the effect of the bias current on the weak

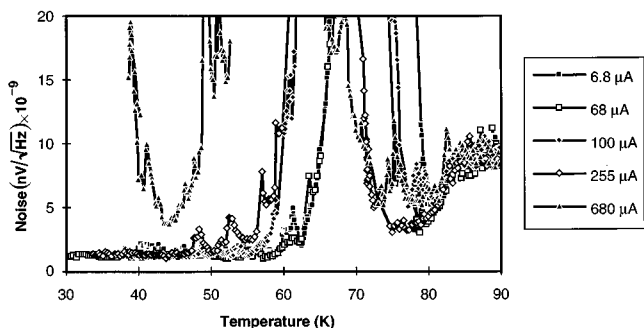


FIG. 4. Noise voltage vs temperature of sample 064-02b, on MgO, at 10 kHz for 6.8, 68, 100, 250, and 680  $\mu\text{A}$  bias currents.

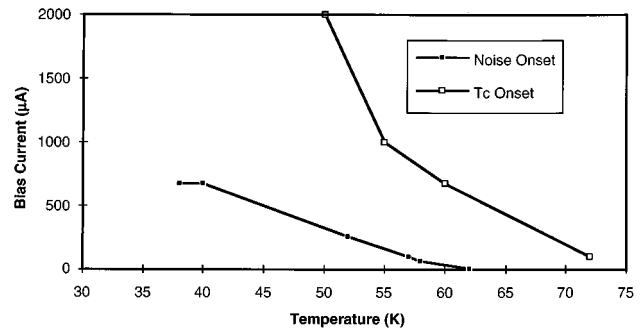


FIG. 5. The onset temperature of the excess noise for sample no. 064-02b, on MgO, vs bias current, and  $T_{c \text{ onset}}$  vs bias current.

links in the film. This should also occur with increasing magnetic field, and such behavior has been reported.<sup>29</sup>

The onset temperature of the excess noise at or below  $T_{c \text{ zero}}$  for sample no. 064-02b as a function of bias current, from the data in Fig. 4, is given in Fig. 5. The values of  $T_{c \text{ onset}}$  for the sample were obtained from the  $R$  vs  $T$  curves measured with different bias currents. The onset temperature of this noise versus bias current is related to the critical current density  $J_c$  versus temperature, and Fig. 5 shows such a correlation. Based on the above discussion, this noise source should exist even at zero bias currents, where the normal regions are mainly determined by the temperature. This is observed in the noise measurements versus temperature, at very low bias current, close to 6.8  $\mu\text{A}$  ( $10^2 \text{ A}/\text{cm}^2$ ), which is the lowest current at which our measurements could be done.

### C. Type (iii) noise

There was another noise characteristic observed at temperatures right below  $T_{c \text{ zero}}$  in sample no. 064-03b, which is less granular than sample 064-02b [scanning electron microscopy (SEM) pictures in Ref. 1]. This kind of noise peaks right below the onset temperature of the excess noise. Figure 6 shows the noise versus temperature of this sample. As shown in the figure, the sample has excess noise similar to that of sample 064-02b, which was associated with the long tail of the  $R$  vs  $T$  curve due to the granularity of that sample. Hence, as shown in Fig. 6, the noise peak below  $T_{c \text{ zero}}$  increases with increasing bias current, but approaches zero

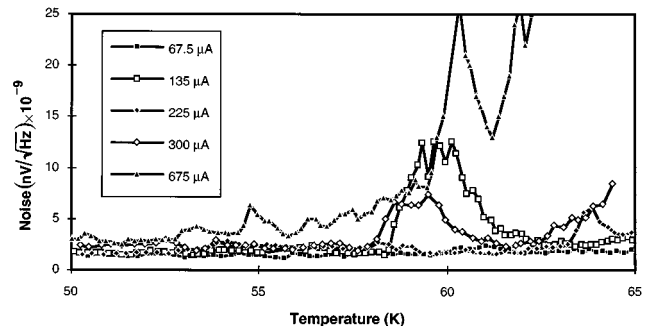


FIG. 6. Noise voltage vs temperature of sample 064-03b, on MgO, at 10 kHz for 67.5, 135, 225, 300, and 675  $\mu\text{A}$  bias currents.

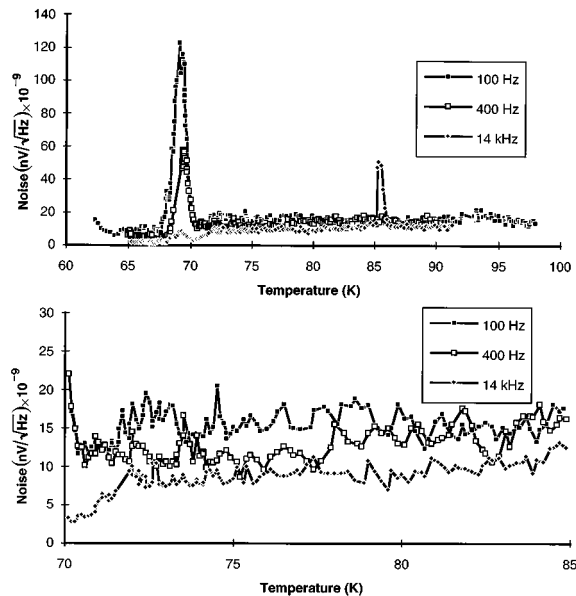


FIG. 7. Noise voltage vs temperature of sample 064-01a, on SrTiO<sub>3</sub>, at 100  $\mu$ A bias current and 100 Hz, 400 Hz, and 14 kHz frequencies.

for zero bias current, and hence differs from the type (ii) noise seen in sample 064-02b. For very large bias currents the excess noise extends over a large region, creating other small peaks, at even lower temperatures.

In the temperature region below  $T_{c \text{ zero}}$ , at low bias currents, a continuous superconducting path is expected to exist between the probes (or current and voltage contacts in the four-probe configuration) of the sample. This fact, and the strong dependence of the noise on the bias current, suggests vortex motion as the source for noise in this region. It can be due to thermally activated two-level or diffusive vortex motion<sup>25,26</sup> that may also be enhanced by a strong Lorentz force due to the applied current.<sup>27,28</sup> This type of noise that peaks below  $T_{c \text{ zero}}$  is also observed for SrTiO<sub>3</sub> substrate sample 064-01a,<sup>1</sup> which is also less granular than sample 064-02b.

#### D. Type (iv) noise

All samples show significant noise in the transition region of temperature between  $T_{c \text{ zero}}$  and  $T_{c \text{ onset}}$ , where  $dR/dT$  is maximum, and the bolometer's  $r_v$  is highest. It is in this region that  $D^*$ , the detectivity of the bolometer, must be maximized. Figures 2, 4, and 7 show noise in this region for two of our samples. Sample 2b on MgO has a relatively wide transition region  $\sim 12$  K, while sample 1a on SrTiO<sub>3</sub> has a transition region of  $\sim 3$  K. They also differ in that the sample on MgO is more granular. Figure 7 shows that the noise in the SrTiO<sub>3</sub> sample is much less than for the MgO sample. For frequencies above 10 kHz, even at the highest bias current used (680  $\mu$ A or  $10^4$  A/cm<sup>2</sup>), the noise voltage remains below about 10 nV Hz<sup>-1/2</sup>; however, it increases strongly with decreasing frequency below 400 Hz, and is also current dependent in this frequency range (see Table II). A possible cause of noise in all the samples in the transition region is

conductance fluctuations due to variations in the volume fraction of the superconducting phase in the current path through the material.<sup>24</sup>

#### E. $D^*$ considerations

We have previously reported<sup>30</sup> the spectral response of the sample on SrTiO<sub>3</sub>, in the wavelength range out to 20  $\mu$ m, using bias currents of 970 and 550  $\mu$ A at 400 Hz modulation frequency, and obtained a  $D^*$  of  $\sim 10^6$  cm Hz<sup>1/2</sup>/W. The detailed spectral response depends upon the absorption and reflection properties of the superconducting film, and the substrate material.<sup>33-38</sup>

To obtain a  $D^*$  of  $\sim 10^6$  cm Hz<sup>1/2</sup>/W at 400 Hz modulation frequency, we note that from Fig. 7  $V_n$  is on the order of 10 nV/Hz<sup>-1/2</sup>, and from Eq. (1), for  $\Delta f=1$  Hz and  $A=9.5 \times 10^{-3}$  cm<sup>2</sup> from Table I, a  $r_v$  of roughly 0.1 V/W is needed. Typical values for our samples range from 2 V/W at 1 Hz to 0.1 V/W at 400 Hz with 500  $\mu$ A bias current.<sup>30</sup> In the low-frequency range, but where  $2\pi fC/G \gg 1$ , with  $C$  the effective specific heat,  $G$  the effective thermal conductance of the bolometer,  $r_v$  is

$$r_v \approx \frac{\eta I}{2\pi f C} \frac{dR}{dT}, \quad (4)$$

with  $\eta$  the fraction of the incident power absorbed by the bolometer,  $I$  the dc bias current, and  $dR/dT$  is essentially  $R_{c \text{ onset}}$  divided by the width of the transition  $T_{c \text{ onset}} - T_{c \text{ zero}}$ . In our samples  $dR/dT \sim 10^3$  and  $C$  is the specific heat of the substrate to a depth equal to the thermal diffusion length at high frequencies,<sup>1</sup> or to the total thickness of the substrate at low frequencies.<sup>1</sup> To increase  $D^*$  to say  $10^{10}$  cm Hz<sup>1/2</sup>/W requires a  $r_v$  of  $10^3$  V/W. This means a sharper transition, as well as a finer serpentine pattern and thinner film to increase  $dR/dT$ , a thinner substrate to decrease  $C$ , and high  $I$ . These are not all independent, i.e., if the film is thinner and the pattern finer, then for a given current  $I$  the critical current density may be exceeded. Reasonable estimates<sup>1,16,30</sup> are that one can obtain a factor of about  $10^2 - 10^3$  from  $dR/dT$  by a sharper transition, thinner films, and a finer pattern, with a critical current density on the order of  $10^6$  A/cm<sup>2</sup>, while  $C$  can be reduced by a factor of  $10^{-1}$  to  $10^{-2}$  by thinning the substrate under the superconducting pattern, from the 250  $\mu$ m minimum thickness used in our samples to about 10-25  $\mu$ m. The operating temperature should be at the peak of  $dR/dT$ , and the frequency should be chosen to maximize  $r_v/V_n$  at the operating temperature. Since  $r_v$  has regimes where it goes as  $1/f$  and  $1/f^{1/2}$ ,<sup>30,39</sup> and in the temperature range of interest  $V_n \sim 1/f$ , it may be possible to enhance the detectivity by going to high frequencies.

Hence, without any breakthroughs in materials, it should be possible to reach a  $D^*$  of  $10^{10}$  cm Hz<sup>1/2</sup>/W with YBCO bolometers with only engineering changes.

#### IV. CONCLUSIONS AND SUMMARY

The observed noise characteristics in YBCO bolometers show significant differences even when the stoichiometry of the samples is the same. The granularity of the samples ap-

appears to be a major cause for the differences seen, and this in turn is related to the substrate used. Since a superconducting bolometer is operated at the maximum in  $dR/dT$ , the noise characteristics in the transition region, type (iv) noise, are the most important for designing a bolometer with optimal detectivity. The noise observed in other temperature regions can be used to help characterize the deposited films, and as feedback for changing the deposition conditions.

Four distinct types of noise were identified in this study. Type (i) occurs in the normal state above  $T_{c \text{ onset}}$ , types (ii) and (iii) occur below  $T_{c \text{ zero}}$ , but are ascribed to SNS junctions at grain boundaries, and flux flow respectively, while type (iv), which is the only one directly relevant to bolometer design, occurs in the transition region  $T_{c \text{ zero}} < T < T_{c \text{ onset}}$  and is mainly due to variations in the fraction of the material in the normal state along the current path. The dependence of these four types of noise on bias current and frequency are summarized in Table II.

Based upon the definition of the detectivity  $D^*$ , and the dependence of the responsivity  $r_v$  on bias current, frequency, and bolometer dimensions, one can project values for  $D^*$  above  $10^{10} \text{ cm Hz}^{1/2}/\text{W}$ . Such detectors, especially at long wavelengths of  $20 \mu\text{m}$  and beyond, would be superior to existing detectors.

<sup>1</sup>M. Fardmanesh, Ph.D. thesis, Drexel University, 1993.

<sup>2</sup>J. D. Vincent, *Fundamentals of Infrared Detector Operation and Testing* (Wiley, New York, 1990).

<sup>3</sup>M. Tinkham and C. J. Lobb, *Solid State Phys.* **42**, 91 (1988).

<sup>4</sup>B. W. Ricketts, R. Driver, and H. K. Welsh, *Solid State Commun.* **67**, 133 (1988).

<sup>5</sup>L. B. Kiss, P. Svedlindh, L. Lundgren, J. Hudner, H. Ohlsen, L. Stolt, and Z. Gingl, *Physica B* **172**, 441 (1991).

<sup>6</sup>B. H. Moeckly, D. K. Lathrop, and R. A. Buhrum (unpublished).

<sup>7</sup>D. Janik, D. May, H. Wolf, and R. Schneider, *IEEE Trans. Appl. Supercond.* **3**, 2148 (1993).

<sup>8</sup>A. Frenkel, M. A. Saifi, T. Venkatesan, P. England, X. D. Wu, and A. Inam, *J. Appl. Phys.* **67**, 3054 (1990).

<sup>9</sup>P. Dutta and P. M. Horn, *Rev. Mod. Phys.* **53**, 497 (1981); M. B. Weissman, *ibid.* **60**, 537 (1988).

<sup>10</sup>G. Jung, S. Vitale, J. Konopka, and M. Bonaldi, *J. Appl. Phys.* **70**, 5440 (1991).

<sup>11</sup>K. H. Han, M. K. Joo, H. J. Shin, Sung-Ik Lee, and Sung-Ho Suck Salk, *IEEE Trans. Appl. Supercond.* **AS-3**, 2947 (1993).

<sup>12</sup>L. B. Kiss, T. Larsson, P. Svedlindh, H. Ohlsen, M. Ottosson, J. Hudner, and L. Stolt, *Physica C* **207**, 318 (1993).

<sup>13</sup>R. D. Black, L. G. Turner, A. Mogro-Campero, T. C. McGee, and A. L. Robinson, *Appl. Phys. Lett.* **21**, 2233 (1989).

<sup>14</sup>J. Hall, H. Hickman, and T. M. Chen, *Solid State Commun.* **76**, 921 (1990).

<sup>15</sup>R. W. Zindler and R. R. Parsons, *J. Vac. Sci. Technol. A* **10**, 3322 (1992).

<sup>16</sup>P. L. Richards, S. Verghese, T. H. Geballe, and S. R. Spielman, *IEEE Trans. Magn.* **MAG-25**, 1335 (1989).

<sup>17</sup>P. L. Richards, J. Clarke, R. Leoni, Ph. Lerch, S. Verghese, M. R. Beasley, T. H. Geballe, R. H. Hammond, P. Rosenthal, and S. R. Spielman, *Appl. Phys. Lett.* **54**, (1989).

<sup>18</sup>L. B. Kiss, P. Svedlindh, L. Lundgren, J. Hudner, H. Ohlsen, and L. Stolt, *Solid State Commun.* **75**, 747 (1990).

<sup>19</sup>G. Forgacs, L. S. Schulman, L. B. Kiss, P. Svedlindh, and L. Lundgren, *Physica C* **177**, 67 (1991).

<sup>20</sup>M. Celasco, M. Lo Bue, A. Masoero, P. Mazzetti, and A. Stepanescu, *IEEE Trans. Appl. Supercond.* **AS-31**, 111 (1993).

<sup>21</sup>A. Maeda, Y. Nakayama, S. Takebayashi, and K. Uchinokura, *Physica C* **160**, 443 (1989).

<sup>22</sup>A. Maeda, H. Watanabe, I. Tsukada, and K. Uchinokura, in *Noise in Physical Systems and 1/f Fluctuations*, edited by T. Musha, S. Sato, and M. Yamamoto (Ohmsha, Tokyo, 1991), p. 115.

<sup>23</sup>A. E. Khalil, *Physica C* **196**, 357 (1992).

<sup>24</sup>Yi Song, A. Misra, P. P. Crooker, and J. R. Gains, *Phys. Rev. B* **45**, 7574 (1992).

<sup>25</sup>M. J. Ferrari *et al.*, *Phys. Rev. Lett.* **64**, 72 (1990).

<sup>26</sup>C. T. Rogers, K. E. Myers, J. N. Eckstein, and I. Bozovic, *Phys. Rev. Lett.* **69**, 160 (1992).

<sup>27</sup>H. J. Jensen, A. Brass, and A. J. Berlinsky, *Phys. Rev. Lett.* **60**, 56 (1988).

<sup>28</sup>H. J. Jensen, Y. Brechet, and A. Brass, *J. Low Temp. Phys.* **74**, 293 (1989).

<sup>29</sup>E. R. Nowak, N. E. Israeloff, and A. M. Goldman, *Phys. Rev. B* **49**, 10 047 (1994).

<sup>30</sup>M. Fardmanesh, A. Rothwarf, and K. J. Scoles, *IEEE Trans. Appl. Supercond.* **AS-5**, 7 (1995).

<sup>31</sup>M. Fardmanesh, A. Rothwarf, and K. J. Scoles, *J. Appl. Phys.* **77**, 4568 (1995).

<sup>32</sup>M. Tinkham, *Introduction to Superconductivity* (McGraw-Hill, New York, 1975).

<sup>33</sup>Z. M. Zhang, B. I. Choi, T. A. Le, M. I. Flik, M. P. Siegal, and J. M. Phillips, *J. Heat Transfer* **114**, 644 (1992).

<sup>34</sup>Z. M. Zhang, B. I. Choi, M. I. Flik, and A. C. Anderson, *J. Opt. Soc. Am. B* **11**, 2252 (1994).

<sup>35</sup>K. E. Goodson and M. I. Flik, in National Heat Transfer Conference, Minneapolis, MN, July 1991.

<sup>36</sup>M. I. Flik, Z. M. Zhang, K. E. Goodson, M. P. Siegal, and J. M. Phillips, *Phys. Rev. B* **46**, 5606 (1992).

<sup>37</sup>W. G. Spitzer, R. C. Miller, D. A. Kleinman, and L. E. Howarth, *Phys. Rev.* **126**, 1710 (1962).

<sup>38</sup>J. C. Galzerani and R. S. Katiyar, *Solid State Commun.* **41**, 515 (1982).

<sup>39</sup>P. E. Phelan, *J. Therm. Phys. Heat Transfer* **9**, 397 (1995).